Structural and theoretical insights into solvent effects in an iron (III) SCO complex

Raúl Díaz-Torres,[a]† Theerapoom Boonprab,[a] Silvia Gómez-Coca,[b] Eliseo Ruiz,[b] Guillaume Chastanet,[c] Phimphaka Harding[a] and David J. Harding*[a]

[a] Functional Materials and Nanotechnology Centre of Excellence, Walailak University, Thasala, Nakhon Si Thammarat, 80160, Thailand.

[b] Departament de Química Inorgànica i Orgànica, Institut de Recerca de Química Teòrica i Computacional, Universitat de Barcelona, Diagonal 645, 08028 Barcelona, Spain.

[c] Université de Bordeaux, ICMCB, 87 avenue du Dr A. Schweitzer, Pessac, F-33608, France.

† Now at Thammasat University Research Unit in Multifunctional Crystalline Materials and Applications (TU-MCMA), Faculty of Science and Technology, Thammasat University, Pathum Thani 12121, Thailand

E-mail: hdavid@mail.wu.ac.th or kphimpha@mail.wu.ac.th

Contents Page No.

Table S1 Selected Fe-N/O bond length (Å), volume cell (Å^3) and octahedral distortion parameters at various temperatures for all compounds.

	1		**2**		**3**	
	$[Fe(qsal\text{-}Cl)_2]NO_3 \cdot MeOH$		$[Fe(qsal\text{-}Cl)_2]NO_3 \cdot EtOH$		$[Fe(qsal\text{-}Cl)_2]NO_3 \cdot 1\text{-}PrOH$	
	150 K	**280 K**	**150 K**	**280 K**	**150 K**	**280 K**
Fe1-O1ph	1.880(2)	1.871(2)	1.885(5)	1.905(3)	1.858(2)	1.860(2)
Fe1-O2ph	1.868(2)	1.863(2)	1.885(5)	1.903(3)	1.883(2)	1.879(2)
Fe1-Oph$_{av}$	1.874	1.867	1.885	1.904	1.870	1.869
Fe1-N1quin	1.969(2)	1.968	1.996(5)	2.126(3)	1.982(2)	1.983(2)
Fe1-N2im	1.936(2)	1.933	1.965(5)	2.108(3)	1.956(3)	1.945(3)
Fe1-N3quin	1.968(2)	1.970	1.980(5)	2.143(3)	1.975(3)	1.995(2)
Fe1-N4im	1.940(2)	1.925	1.960(5)	2.104(3)	1.941(3)	1.962(3)
Fe1-N$_{av}$	1.953	1.949	1.975	2.120	1.963	1.971
Fe2-O3ph	1.884(2)	1.894	-	-	-	-
Fe2-O4ph	1.869(2)	1.882	-	-	-	-
Fe2-Oph$_{av}$	1.876	1.888	-	-	-	-
Fe2-N5quin	1.994(10)	2.076	-	-	-	-
Fe2-N6im	1.944(3)	2.041	-	-	-	-
Fe2-N7quin	1.983(9)	2.069	-	-	-	-
Fe2-N8im	1.937(3)	2.040	-	-	-	-
Fe2-N$_{av}$	1.964	2.056	-	-	-	-
V / Å^3	2984	3065	3034	3125	6296	6428
Σ-Fe1, Fe2	46, 51	46, 52	50	69	51	51
Θ-Fe1, Fe2	114, 155	117, 181	135	225	134	135

	2ns [Fe(qsal-Cl)$_2$]NO$_3$		
	360 K	**320 K**	**200 K**
Fe1-O1ph	1.905(2)	1.888(2)	1.882(2)
Fe1-O2ph	1.891(2)	1.871(2)	1.870(1)
Fe1-Oph$_{av}$	1.898	1.879	1.876
Fe1-N1quin	2.116(2)	2.024(2)	1.970(2)
Fe1-N2im	2.083(3)	1.993(2)	1.948(2)
Fe1-N3quin	2.117(2)	2.026(2)	1.981(2)
Fe1-N4im	2.081(3)	1.991(2)	1.947(2)
Fe1-N$_{av}$	2.100	2.001	1.961
V / Å^3	2854	2816	2761
Σ-Fe1	62	47	48
Θ-Fe1	193	137	123

Table S2 Crystallographic data and structure refinement of all compounds.

	1 $[Fe(qsal\text{-}Cl)_2]NO_3 \cdot MeOH$		**2** $[Fe(qsal\text{-}Cl)_2]NO_3 \cdot EtOH$		**3** $[Fe(qsal\text{-}Cl)_2]NO_3 \cdot 1\text{-}PrOH$	
	150 K	**280 K**	**150 K**	**280 K**	**150 K**	**280 K**
Empirical formula	$C_{33}H_{24}Cl_2FeN_5O_6$	$C_{33}H_{24}Cl_2FeN_5O_6$	$C_{34}H_{26}Cl_2FeN_5O_6$	$C_{34}H_{26}Cl_2FeN_5O_6$	$C_{35}Cl_2FeH_{28}N_5O_6$	$C_{35}Cl_2FeH_{28}N_5O_6$
Formula weight/ gmol^{-1}	713.32	713.32	727.366	727.366	741.37	741.37
Crystal system	triclinic	triclinic	monoclinic	monoclinic	monoclinic	monoclinic
Space group	$P\bar{1}$	$P\bar{1}$	$P2_1/c$	$P2_1/c$	$I2/a$	$I2/a$
a / Å	10.27985(17)	10.27045(20)	9.7517(2)	9.86853(18)	19.1751(3)	19.3217(2)
b / Å	12.74528(15)	12.7798(2)	25.8966(4)	25.6178(4)	11.0201(2)	11.0517(2)
c / Å	23.5809(3)	24.3948(4)	12.1742(1)	12.45218(18)	29.7982(5)	30.1028(5)
α / °	94.8650(10)	96.6399(13)	90	90	90	90
β / °	99.1577(12)	100.2941(14)	99.275(1)	96.8585(16)	90.4220(10)	90.3700(10)
γ / °	99.9168(12)	100.1584(16)	90	90	90	90
V	2984.54(7)	3064.99(9)	3034.23(8)	3125.52(9)	6296.53(18)	6427.95(17)
Z	4	4	4	4	8	8
Absorption coefficient / mm^{-1}	6.185	6.023	6.096	5.918	5.887	5.767
Reflections collected	46286	34803	23307	49448	24396	25999
Independent reflections, R_{int}	10931, 0.0642	7701, 0.1016	5553, 0.0509	5694, 0.0598	5757, 0.0381	5880, 0.0282
Max. and min. transmission	-	-	-	-	-	-
Restrains/parameters	70/1070	36/851	21/474	6/415	21/417	20/417
Final R indices [I>=2σ (I)]	0.0480	0.0618	0.0729	0.0738	0.0568	0.0560
R_1, wR_2	0.1287	0.1687	0.2040	0.1978	0.1584	0.1747
CCDC No.	2175688	2175687	2175689	2175690	2175691	2175692

	2ns $[Fe(qsal\text{-}Cl)_2]NO_3$		
	360 K	**320 K**	**200 K**
Empirical formula	$C_{32}H_{20}Cl_2FeN_5O_5$	$C_{32}H_{20}Cl_2FeN_5O_5$	$C_{32}H_{20}Cl_2FeN_5O_5$
Formula weight/ gmol^{-1}	681.28	681.28	681.28
Crystal system	monoclinic	monoclinic	monoclinic
Space group	$P2_1/n$	$P2_1/n$	$P2_1/n$
a / Å	13.6679(2)	13.3494(3)	13.13396(19)
b / Å	15.2712(2)	15.3915(3)	15.36840(17)
c / Å	14.5271(2)	14.4332(3)	14.35516(19)
α / °	90	90	90
β / °	109.7236(19)	108.239(2)	107.6913(15)
γ / °	90	90	90
V	2854.28(8)	2816.56(10)	2760.52(7)
Z	4	4	4
Absorption coefficient / mm^{-1}	6.412	6.498	6.630
Reflections collected	22988	21258	21967
Independent reflections,	5307	5240	0.0443
R_{int}	0.0473	0.0509	
Max. and min.	0.853	1.000	0.708
transmission	0.573	0.514	0.537
Restrains/parameters	18/406	18/406	0/406
Final R indices [I>=2σ (I)]	0.0496	0.0435	0.0371
R_1, wR_2	0.1435	0.1108	0.1009
CCDC No.	2175695	2175693	2175694

Table S3 Intermolecular interactions of all compounds (Å).

		1 $[Fe(qsal\text{-}Cl)_2]NO_3\cdot MeOH$		2 $[Fe(qsal\text{-}Cl)_2]NO_3\cdot EtOH$		3 $[Fe(qsal\text{-}Cl)_2]NO_3\cdot 1\text{-}PrOH$	
		150 K	**280 K**	**150 K**	**280 K**	**150 K**	**280 K**
1D chains							
Fe-Fe							
	π-π (Type A – Fe1-Fe1)	3.295	3.259	3.363	3.386	3.373	3.345
	π-π (Type B – Fe2-Fe2)	3.221	3.368	-	-	-	-
	π-π (Type C – Fe1-Fe2)	3.339	3.293	-	-	-	-
	C-H···O	2.484	2.616	2.467	2.457	-	-
	C-H···O	2.645	2.722	2.580	2.703	-	-
	C-H···Cl	2.869	2.904	-	-	3.281	3.296
	Fe-Fe (Type A)	6.856	6.926	7.161	7.044	7.011	7.061
	Fe-Fe (Type B)	7.774	7.654	6.984	7.044	10.330	9.368
ROH	OH_e···C-H	2.539	2.681	2.704	**	**	**
	OH_e···ON	2.159	2.501	2.051	**	**	**
NO_3	O···C-H	2.516	2.675	2.576	2.592	2.549	2.601*
2D plane							
	π-π	3.484	3.471*	-	-	-	-
	C-H···Cl	3.098	3.073	3.017	3.061	3.275	3.285
	O···Cl	3.114	3.229	-	-	-	-
	P4AE (CH···$C_{centroid}$)	-	-	-	-	2.830	2.909
	P4AE (π-π, quin-quin)	-	-	-	-	3.497	3.526
NO_3	NO···CH	2.380	2.378	2.576	2.534	2.538	2.395

3D structure							
	C-H···Cl	2.960	3.073*	3.017	3.061	-	-
NO_3	NO···CH	2.286	2.378	2.605	2.608	2.606	2.713

*Disorder in the group
** Solvent mask used in the refinement.

		2ns $[Fe(qsal\text{-}Cl)_2]NO_3$		
		360 K	**320 K**	**200 K**
1D chains				
Fe-Fe				
	π-π (Type A – Fe1-Fe1)	3.499	3.477	3.459
	π-π (Type B – Fe2-Fe2)	-	-	-
	π-π (Type C – Fe1-Fe2)	-	-	-
	C-H···O	2.701	2.647	2.583
	Cl···O	3.170	3.225	3.202
	Fe-Fe (Type A)	6.760	6.906	6.930
	Fe-Fe (Type B)	10.398	10.515	10.529
NO_3	O···C-H	2.681	2.537	2.450
2D plane				
NO_3	NO···CH	2.477	2.409	2.348
3D structure				
	C-H···Cl	2.898	2.863	2.807
	C-H···π	2.592	2.560	2.524
	π-π	3.362	3.351	3.311
NO_3	NO···CH	2.493	2.552	2.369

Table S4 Distances between the chains (d_{chain}) and the planes (d_{plane}) at different temperatures.

	T = 150 K		T = 280 K	
	d_{chain} (Å)	d_{plane} (Å)	d_{chain} (Å)	d_{plane} (Å)
1 $[Fe(qsal\text{-}Cl)_2]NO_3 \cdot MeOH$	12.475	10.280	12.780	10.270
2 $[Fe(qsal\text{-}Cl)_2]NO_3 \cdot EtOH$	9.752	13.687	9.869	13.696
3 $[Fe(qsal\text{-}Cl)_2]NO_3 \cdot 1\text{-}PrOH$	11.020	18.611	11.052	18.769
	T = 200 K		T = 360 K	
2ns $[Fe(qsal\text{-}Cl)_2]NO_3$	15.368	14.355	15.271	14.527

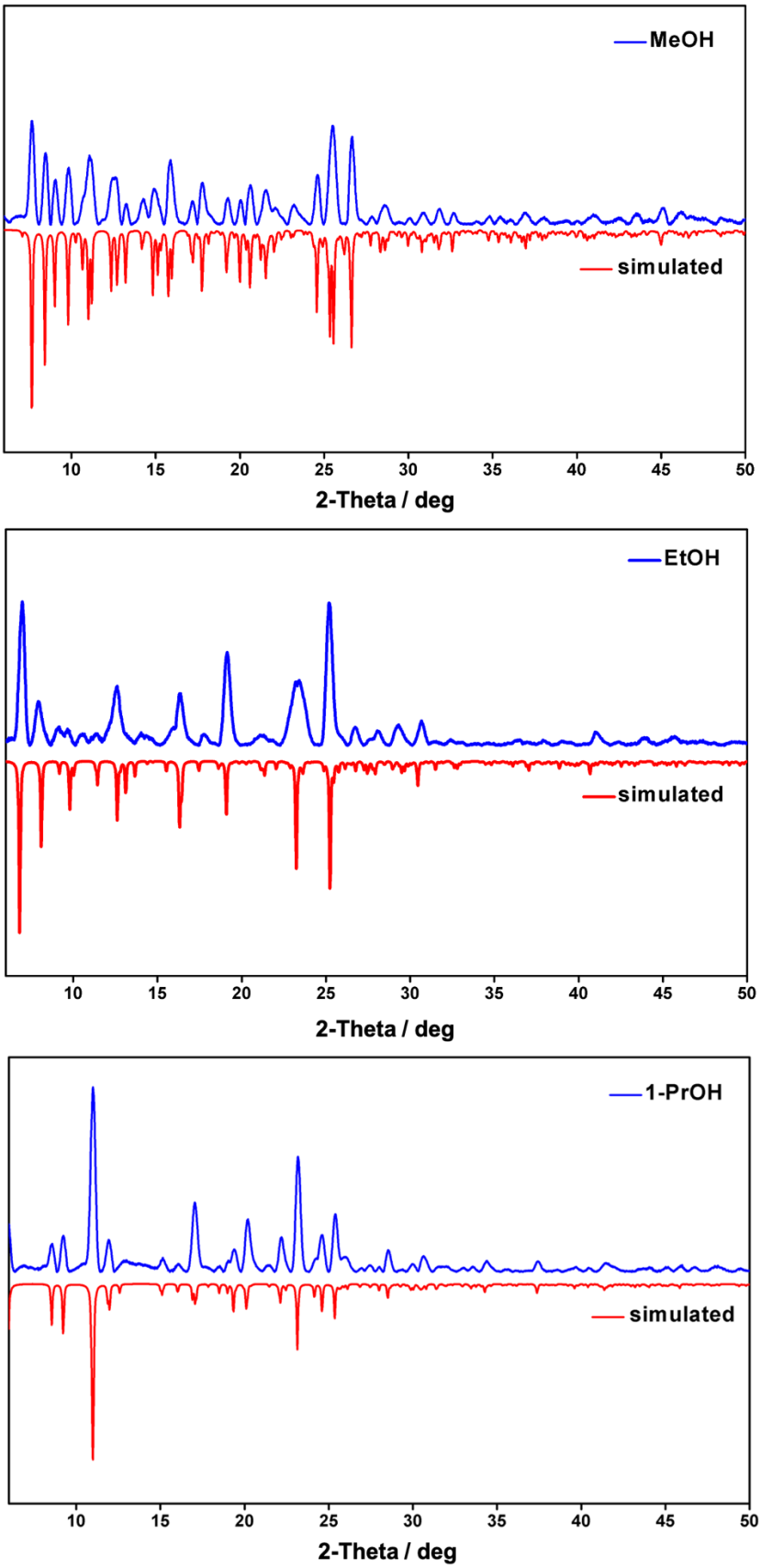

Figure S1. Experimental PXRD diffractograms (blue) and the corresponding simulated patterns (red) for **1**-**3**.

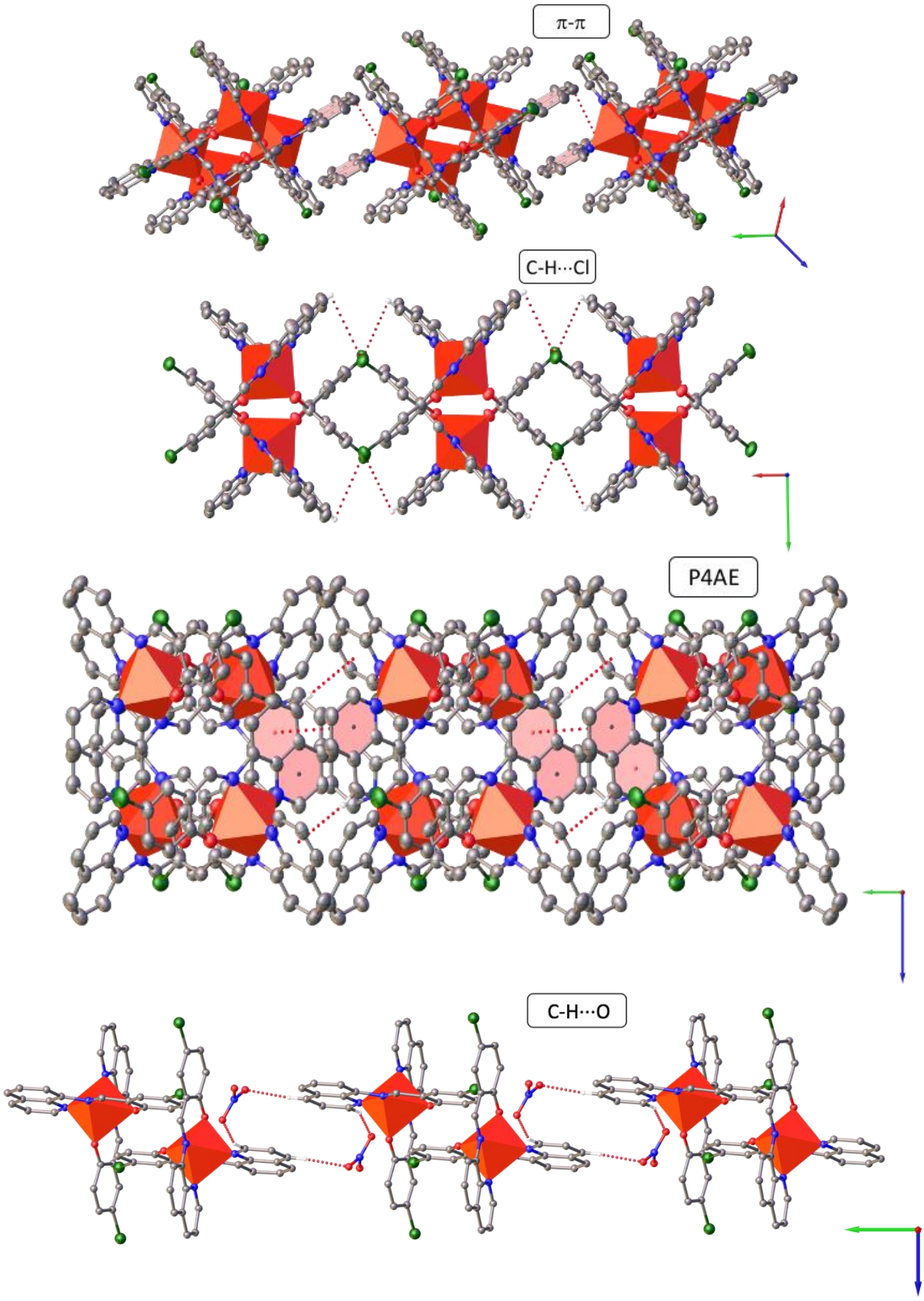

Figure S2. Structure representation of the 2D supramolecular interactions connecting the chains of iron (III) for **1** (top), **2** (middle-top), **3** (middle-bottom) and **2ns** (bottom) at 150 K (**1**-**3**) and 200 K (**2ns**).

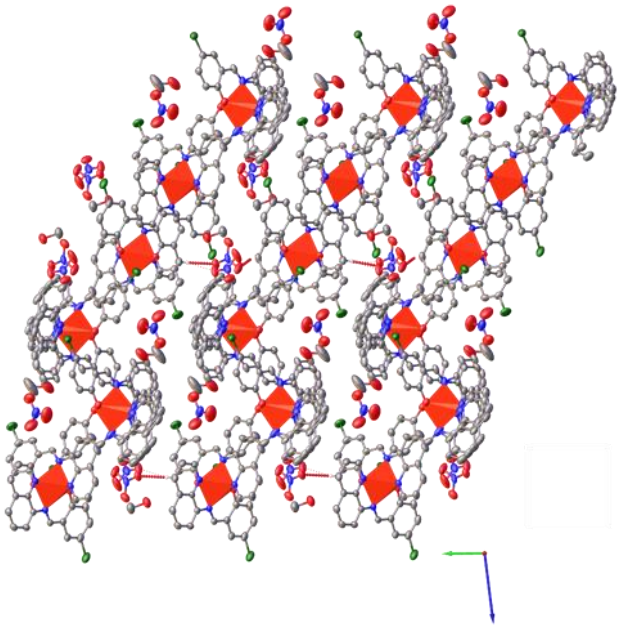

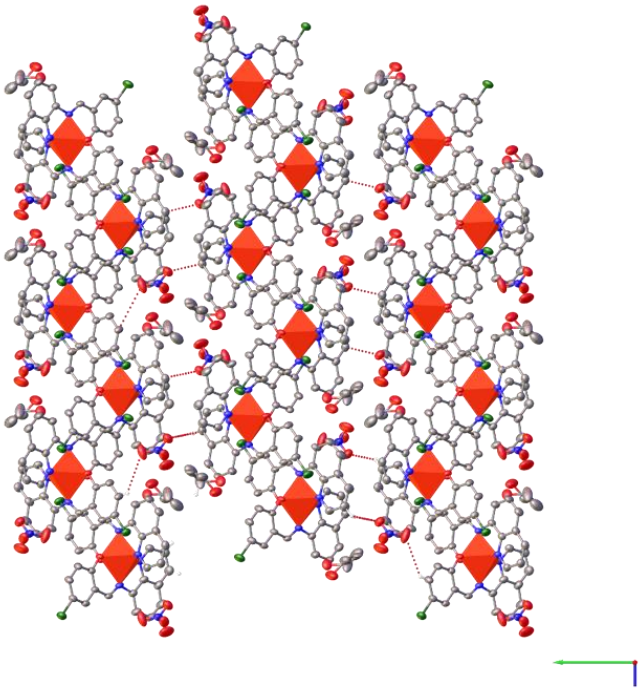

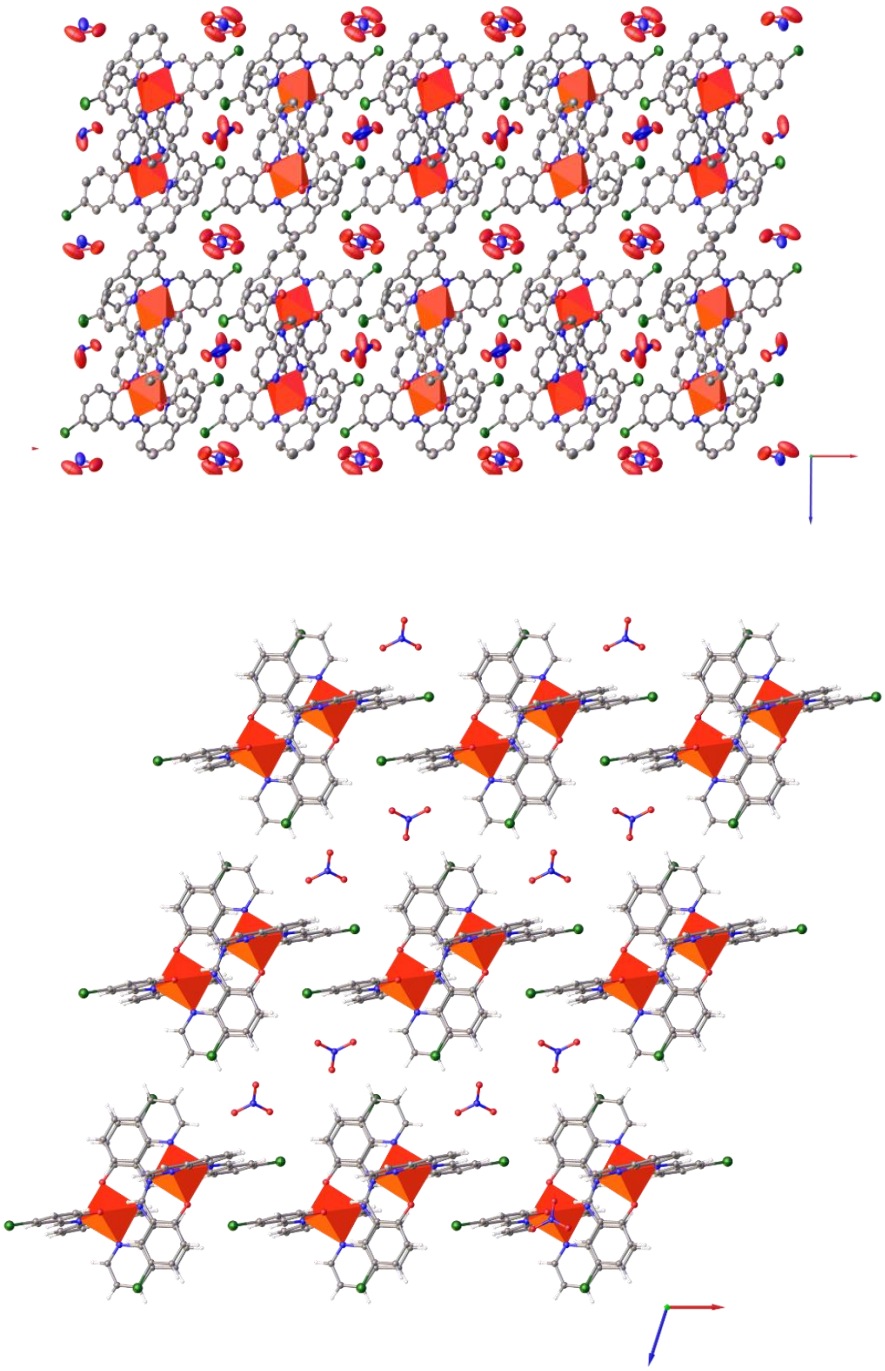

Figure S3. Structure representation of the 3D structure connecting the planes by nitrate molecules for **1** (top), **2** (middle-top), **3** (middle-bottom) and **2ns** (bottom) at 150 K (**1-3**) and 200 K (**2ns**).

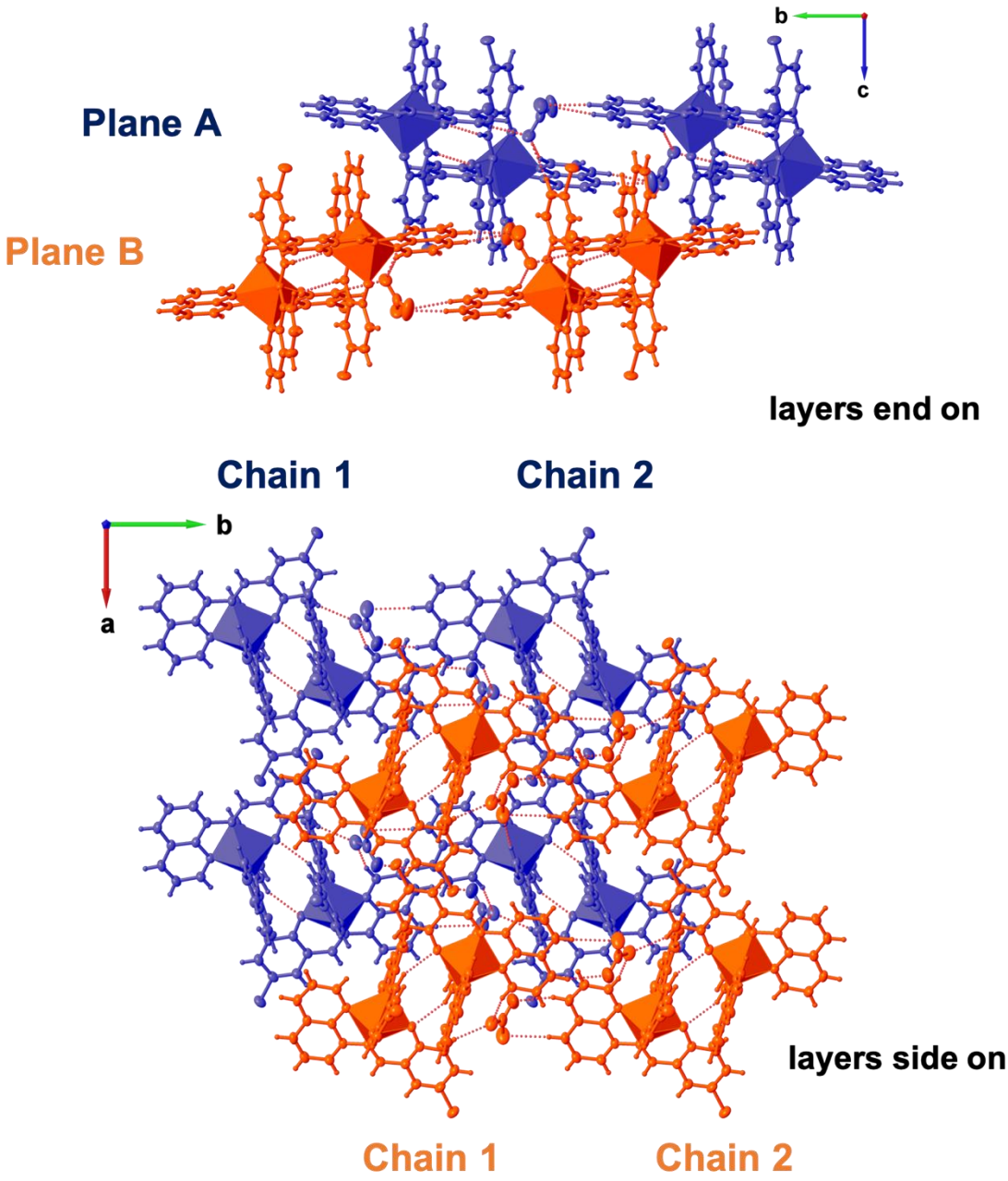

Figure S4. Structure representation of the 3D structure for 2ns with layers end on view (top) and layers side on view (bottom) for **2ns** at 200 K.

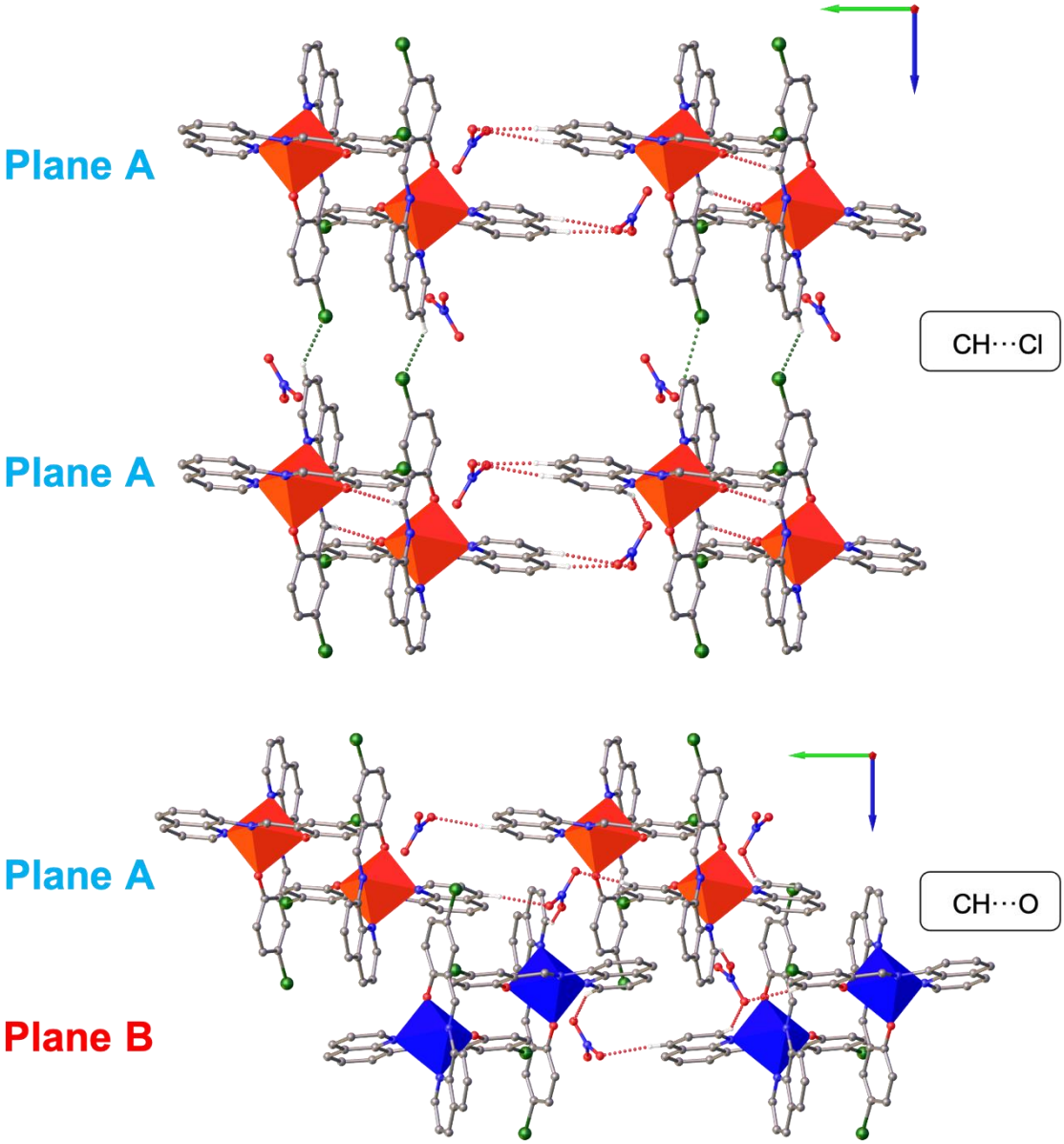

Figure S5. Structure representation of the 3D structure for **2ns** with plane A to plane A interactions and plane A to plane B interactions at 200 K.

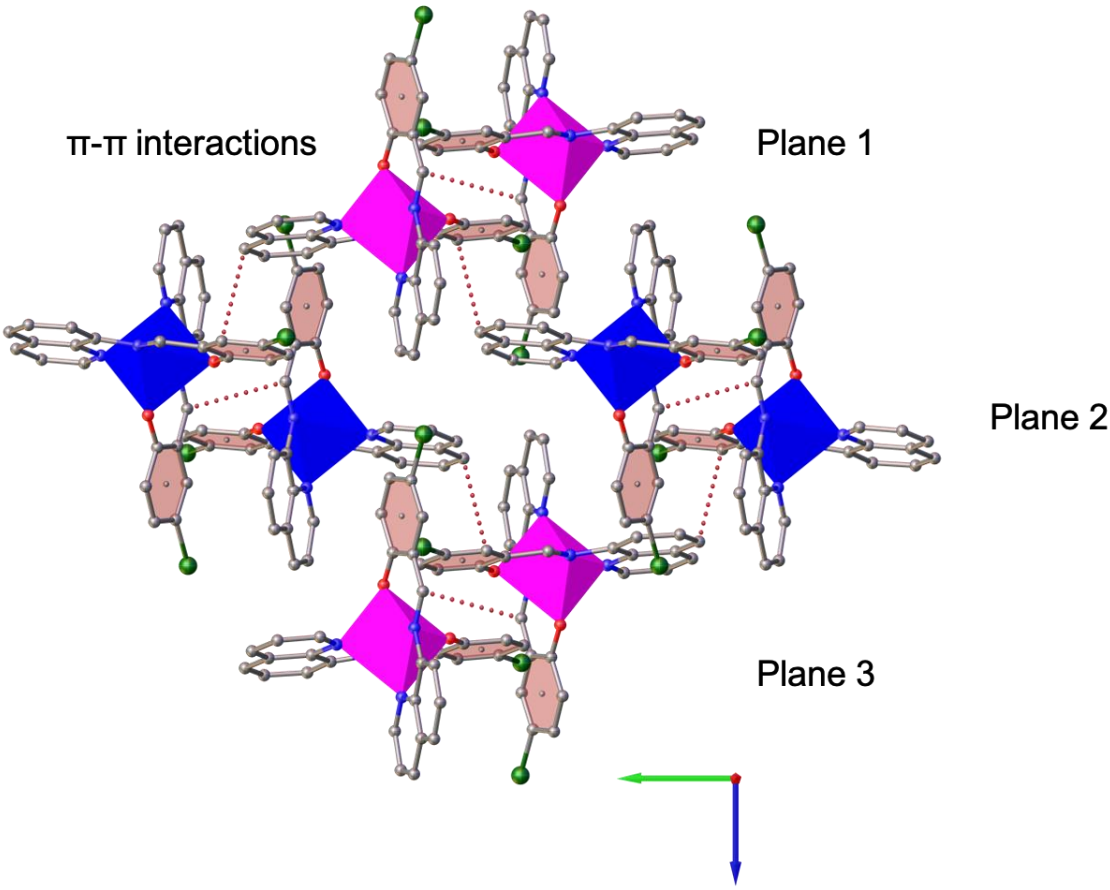

Figure S6. Structure representation of the 3D structure connecting the planes by π-π interactions for **2ns** at 200 K.

Table S5. Intermolecular interactions contributions for **1-2** calculated by Hirshfeld surface at different temperatures.

Complex	T(K)	H···H	H···Cl	H···O	H···C	C···C	C···Cl	O···Cl	Cl···Cl	Other
1 [Fe(qsal-Cl)$_2$]NO$_3$·MeOH	150	36.7	9.9	20.4	14.3	6.9	8.4	1.3	0	2.1
	280	37.5	10.2	18.9	14.0	6.8	8.5	1.6	0	2.5
2 [Fe(qsal-Cl)$_2$]NO$_3$·EtOH	150	34.0	6.1	24.5	13.9	8.0	9.9	0.6	1.5	2.5
	280*									
2ns [Fe(qsal-Cl)$_2$]NO$_3$	200	27.0	11.8	20.8	21.8	7.8	6.2	2.0	0.0	2.6
	360	26.8	11.8	21.1	20.3	8.5	5.5	2.5	0.0	3.5

*Solvent mask used in the refinement

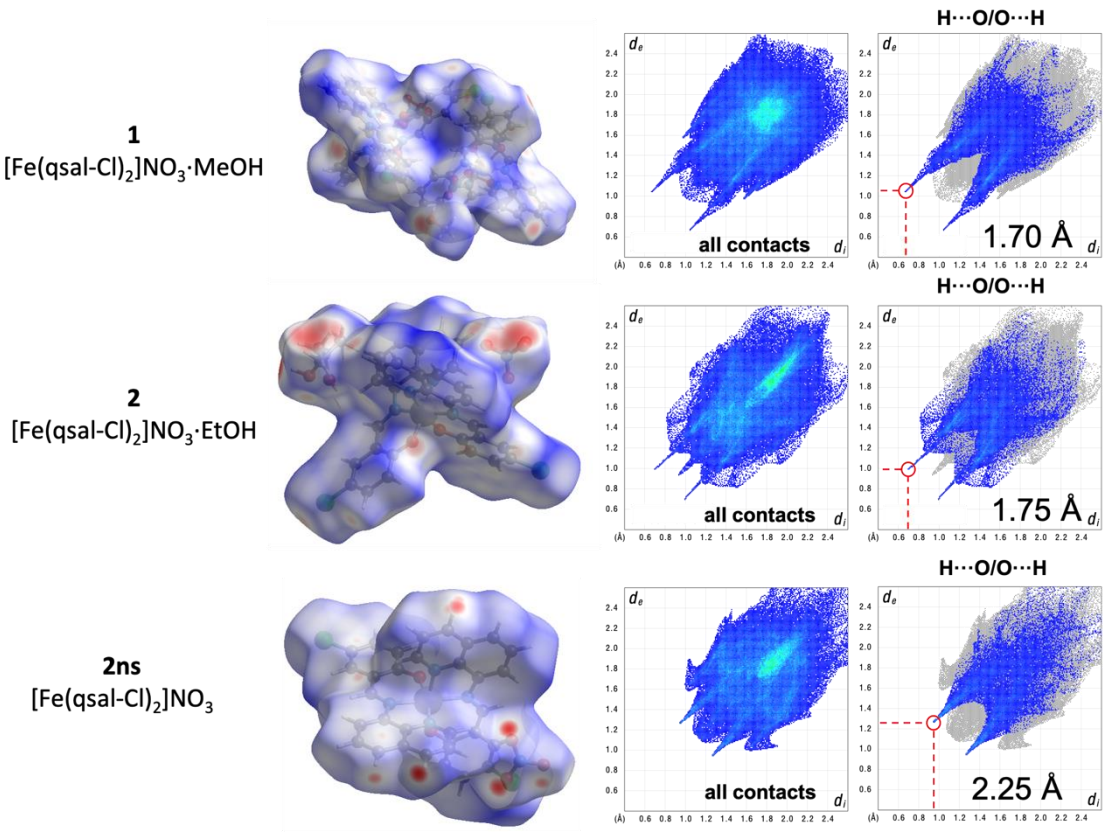

Figure S7. Hirshfeld surface mapped with d_{norm} (left) and 2D fingerprint of all contacts and O···H interactions for **1, 2** and **2n**.

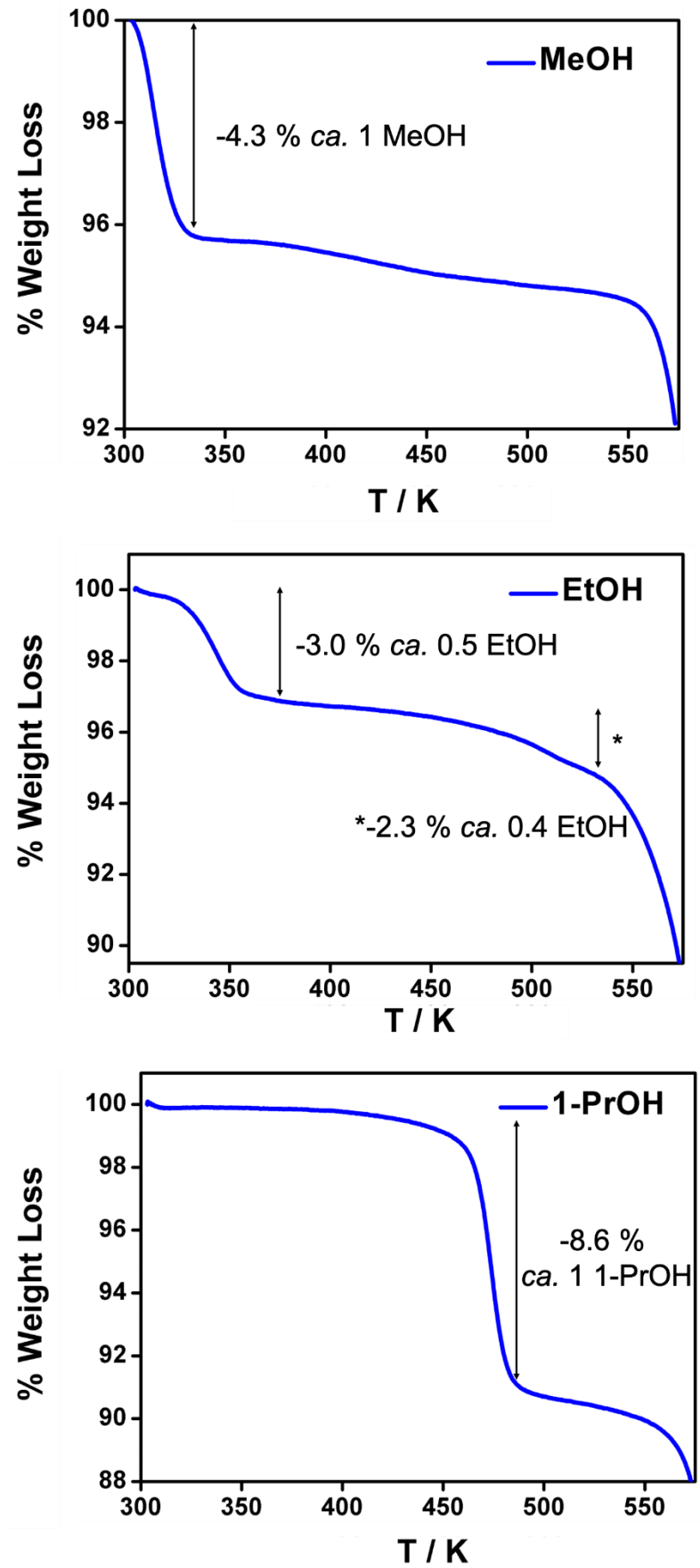

Figure S8. TGA curves for **1-3**, with the assigned mass losses.

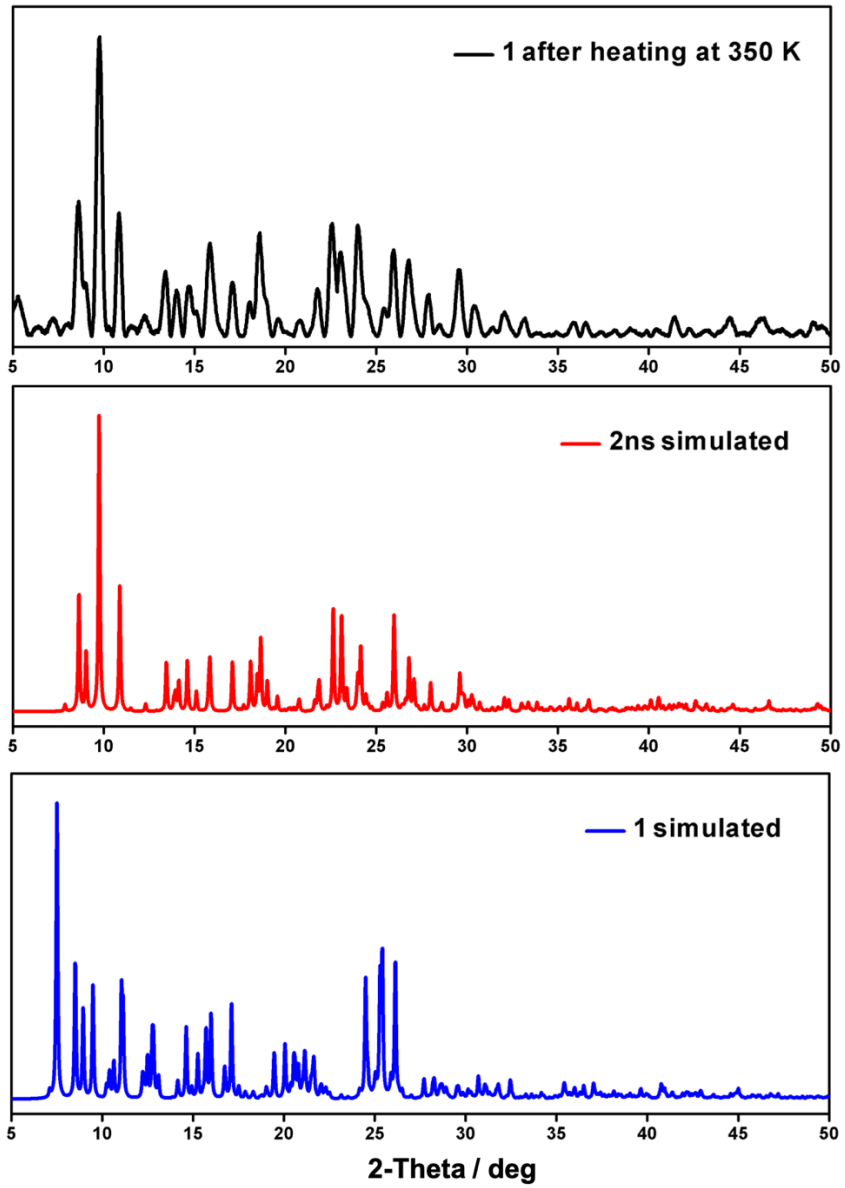

Figure S9. Experimental PXRD diffractogram of **1** after heating at 350 K and the corresponding simulated patterns of solvated complex **1** and **2ns** (non-solvated).

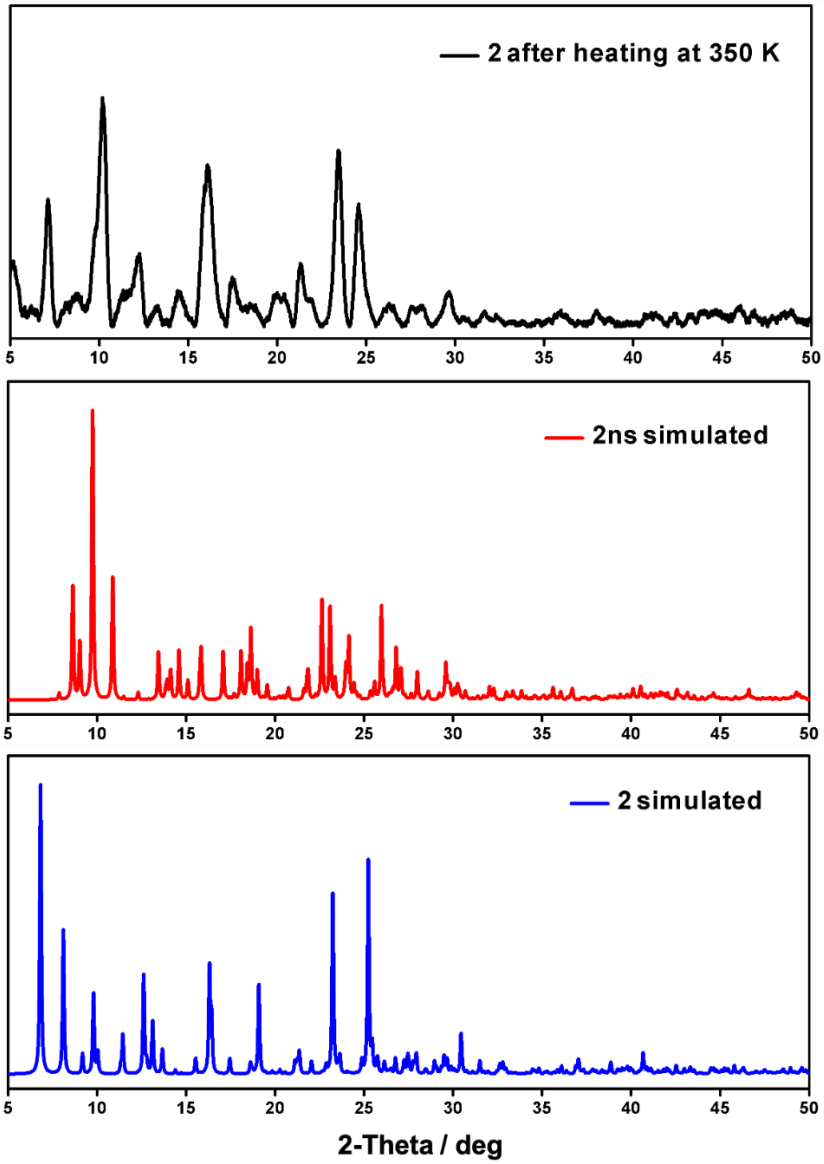

Figure S10. Experimental PXRD diffractogram of **2** after heating at 350 K and the corresponding simulated patterns of solvated complex **2** and **2ns** (non-solvated).

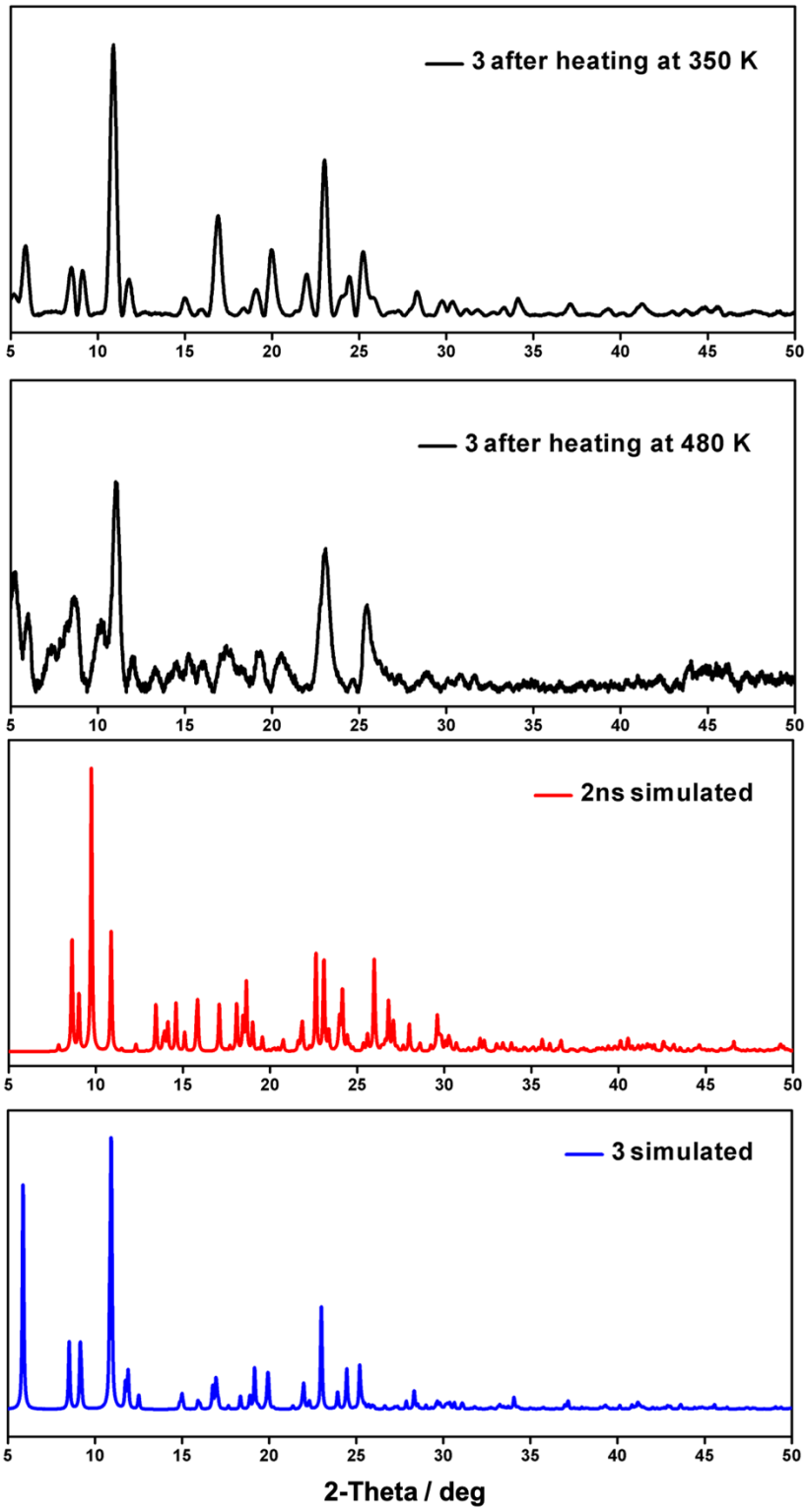

Figure S11. Experimental PXRD diffractogram of **3** after heating at 350 K and 480K, and the corresponding simulated patterns of solvated complex **3** and **2ns** (non-solvated).

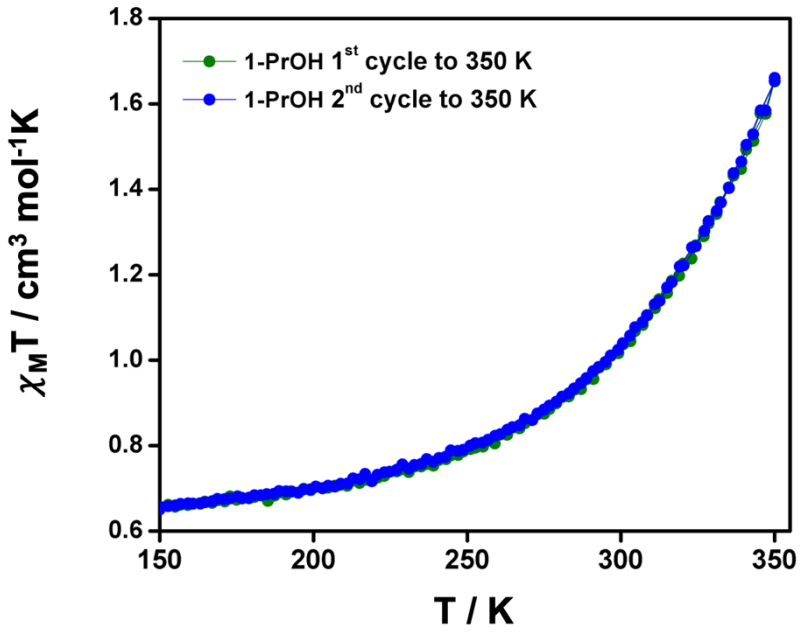

Figure S12. Thermal variation of $\chi_M T$ versus T plots for **3** at different cycles.

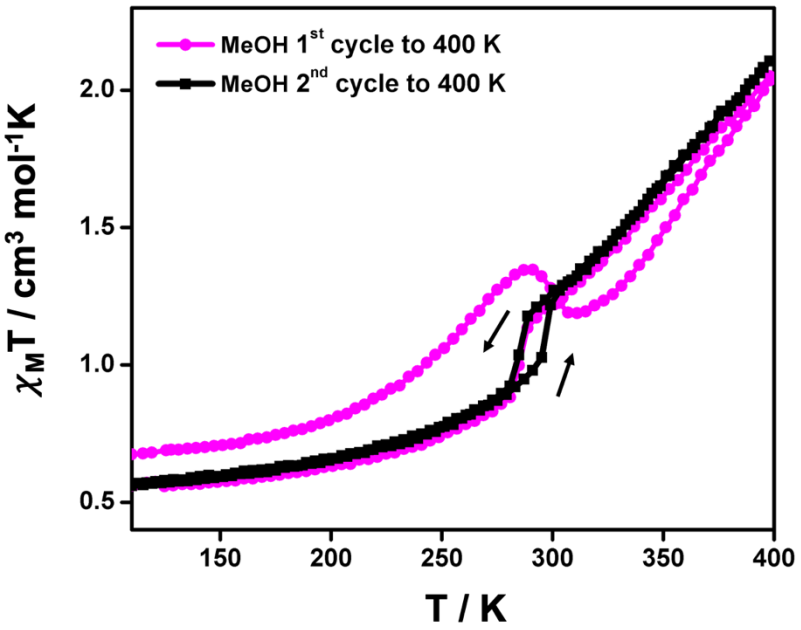

Figure S13. Thermal variation of $\chi_M T$ versus T plots for **1** at different cycles.

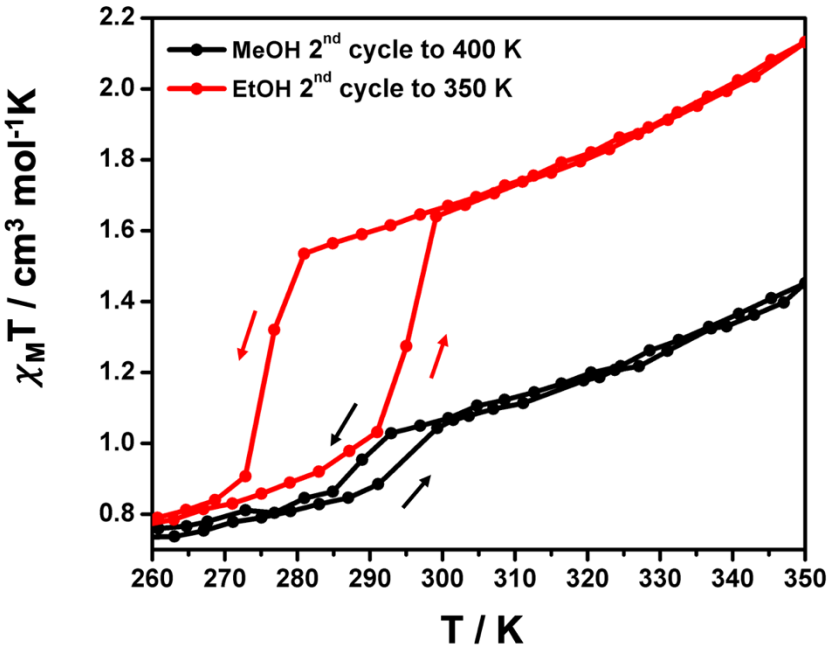

Figure S14. Thermal variation of $\chi_M T$ versus T plots for **1** and **2** at the 2nd cycle.

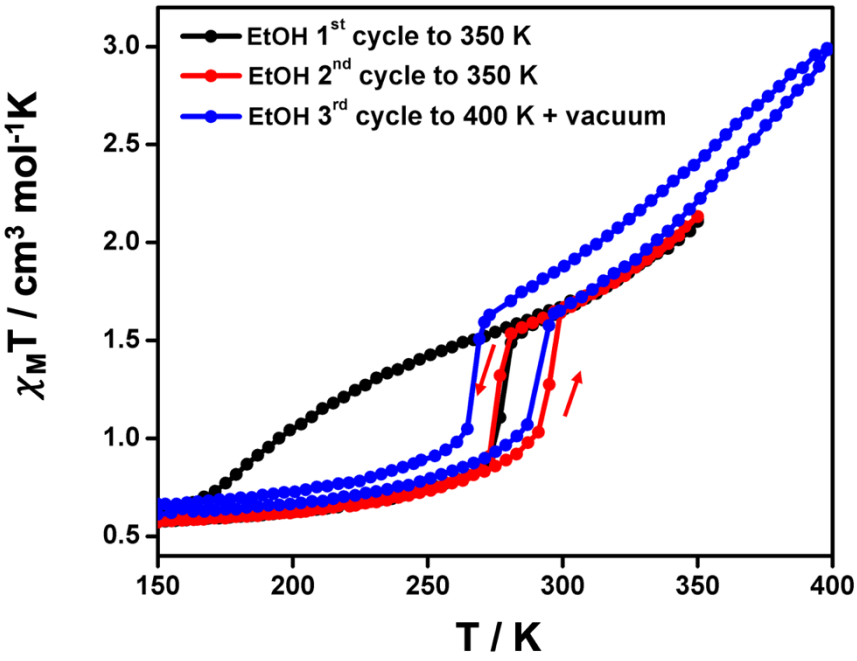

Figure S15. Thermal variation of $\chi_M T$ versus T plots for **2** at different cycles.

Table S6 Comparison of DFT optimized and experimental (in parenthesis) average bond lengths (Å) and volume cells (Å^3) for the low- and high- spin states for compounds **1** and **2**. CIF files of the optimized structures are available as ESI.

	1 $[Fe(qsal\text{-}Cl)_2]NO_3 \cdot MeOH$		**2** $[Fe(qsal\text{-}Cl)_2]NO_3 \cdot EtOH$	
	LS	**HS**	**LS**	**HS**
Fe-Oph$_{av}$	1.901 (1.874)	1.947	1.841 (1.885)	1.946 (1.904)
Fe-N$_{av}$	1.955 (1.953)	2.162	1.909 (1.975)	2.171 (2.120)
volume	2958 (2984)	3036	3021 (3034)	3039 (3125)

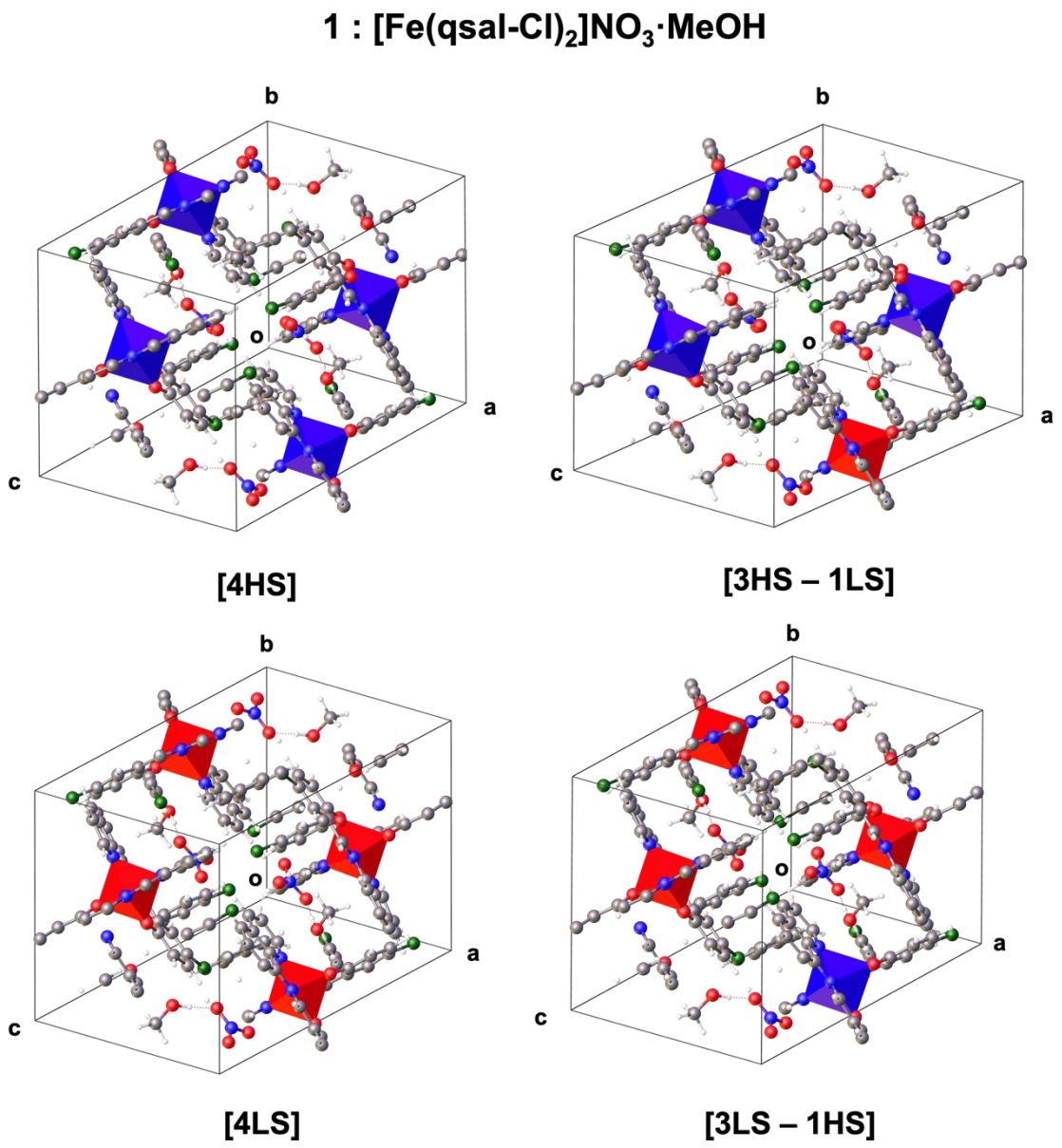

Figure S16. Unit cell of the optimized structures of **1** with [4HS] and [3HS-1LS] (top) [4LS] and [3LS-1HS] (bottom).

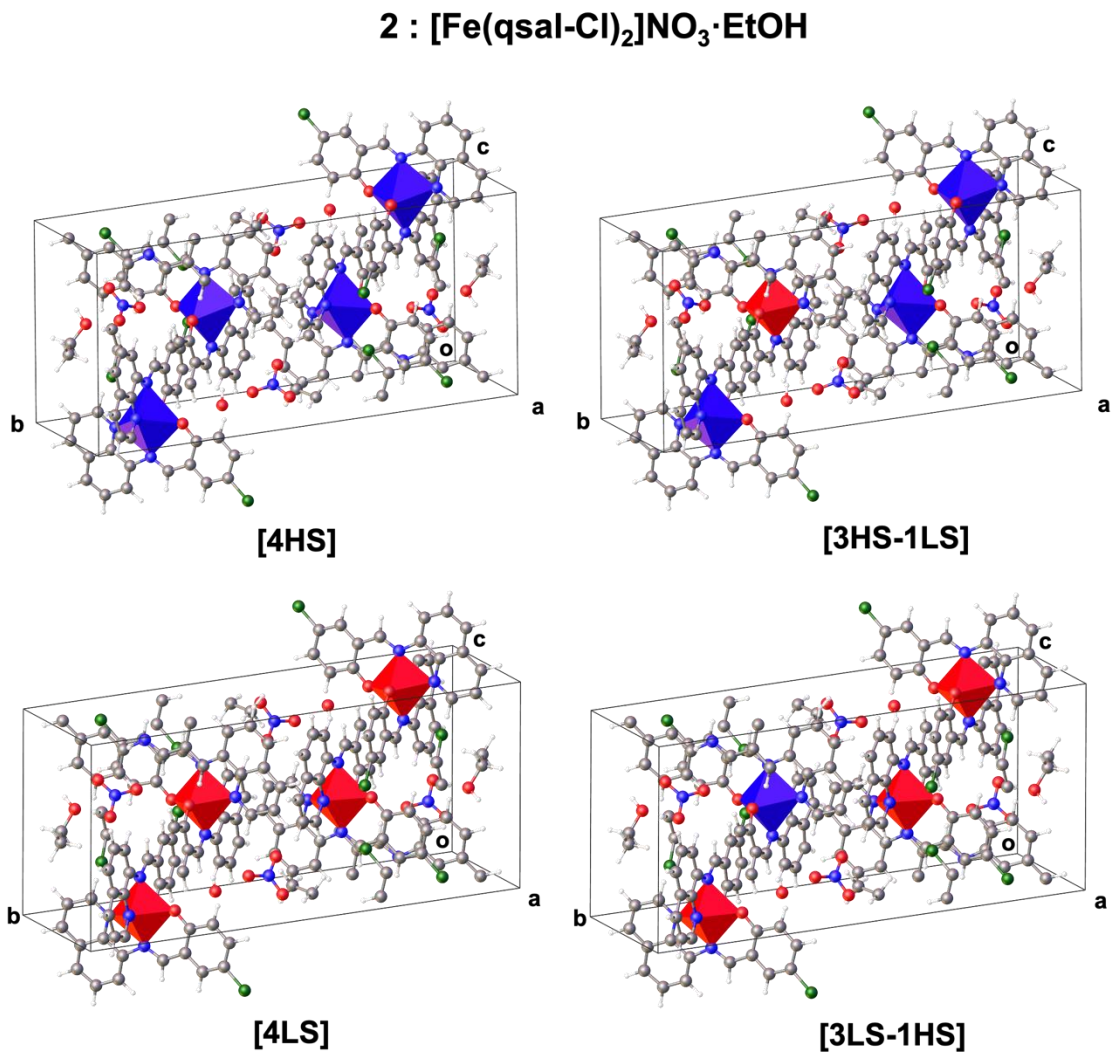

Figure S17. Unit cell of the optimized structures of **2** with [4HS] and [3HS-1LS] (top) [4LS] and [3LS-1HS] (bottom).

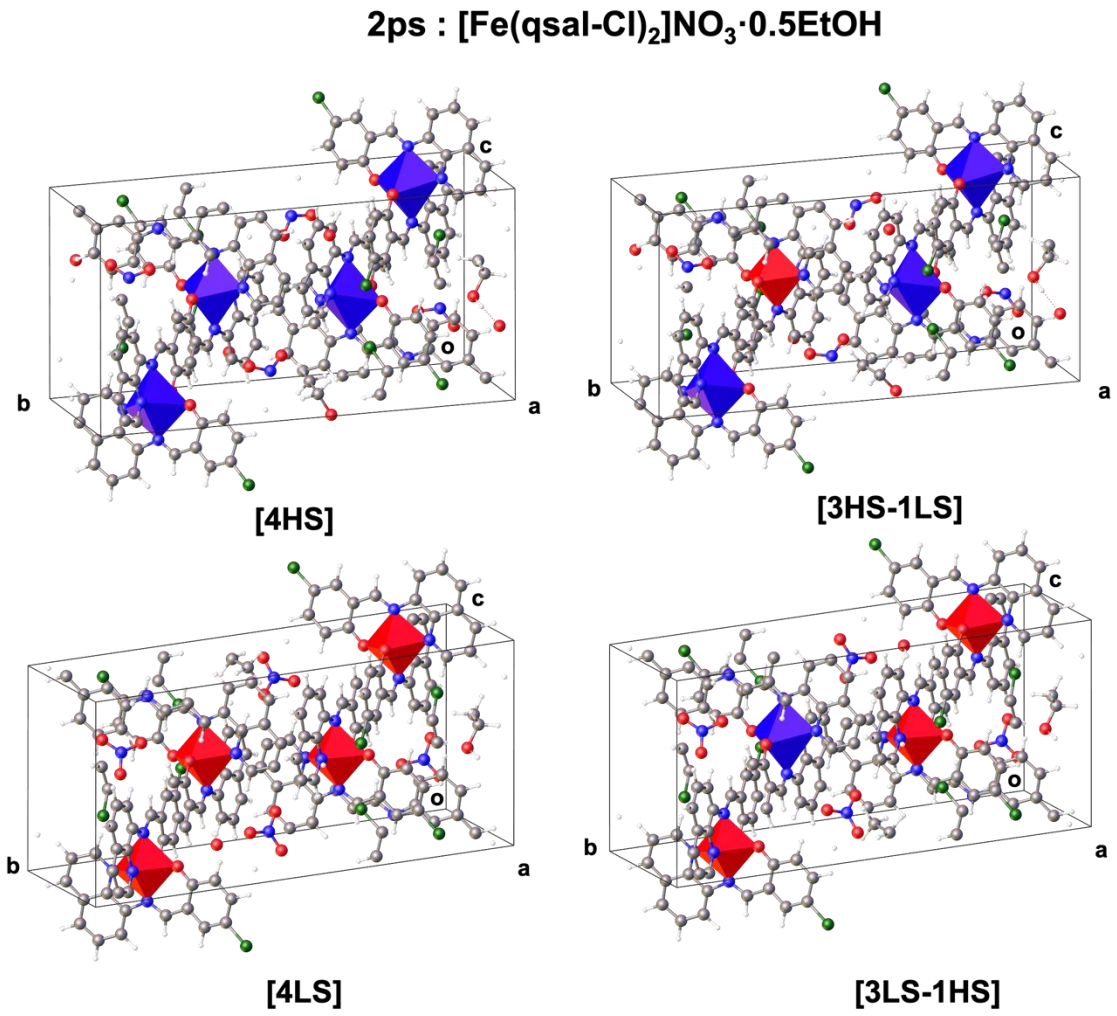

Figure S18. Unit cell of the optimized structures of **2ps** with [4HS] and [3HS-1LS] (top) [4LS] and [3LS-1HS] (bottom).

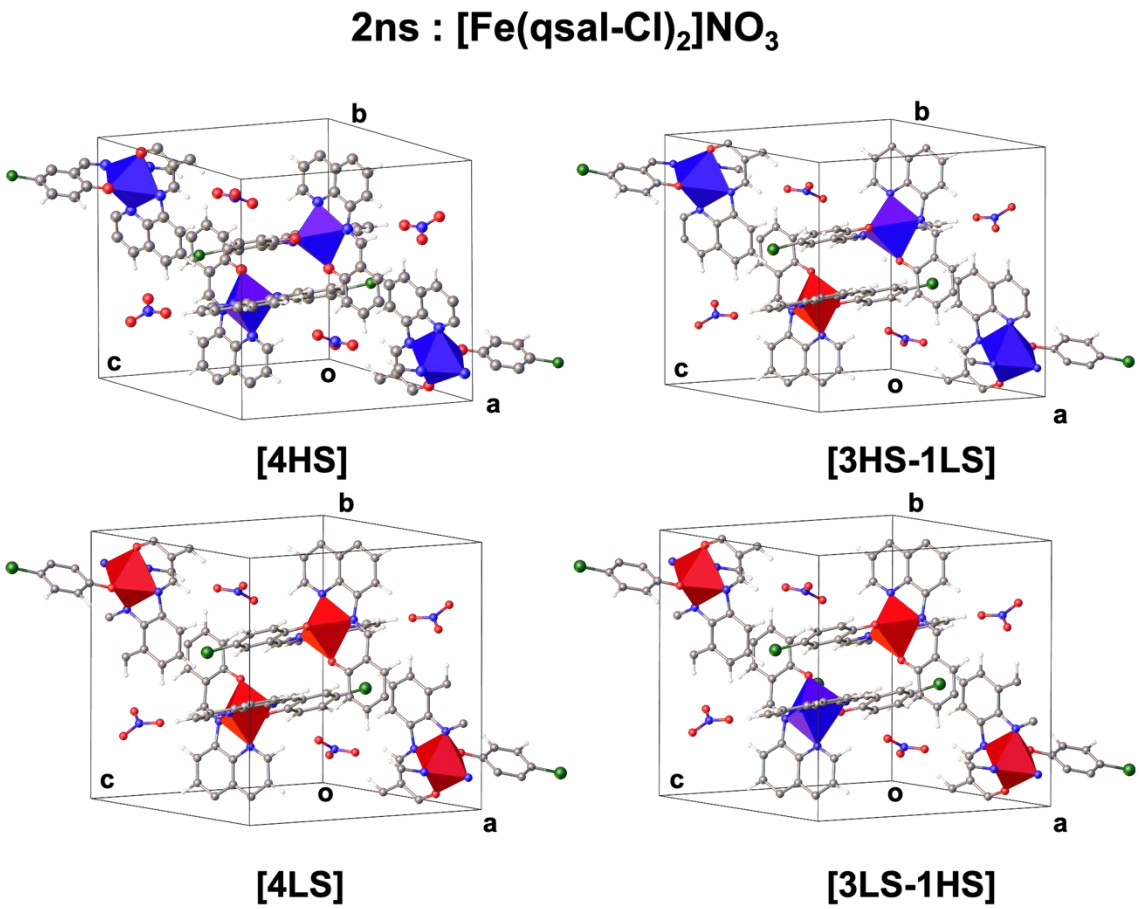

Figure S19. Unit cell of the optimized structures of **2ns** with [4HS] and [3HS-1LS] (top) [4LS] and [3LS-1HS] (bottom).